

This is the author-created version of the following work:

Brice, Sara, Millett, Emma L., and Philippa, Bronson (2022) *The validity of using inertial measurement units to monitor the torso and pelvis sagittal plane motion of elite rowers. Journal of Sports Sciences, 40 (8) pp. 950-958.*

Access to this file is available from:

<https://researchonline.jcu.edu.au/72650/>

© 2022 Informa UK Limited, trading as Taylor & Francis Group. This is an Accepted Manuscript of an article published by Taylor & Francis in Journal of Sports Sciences on 24 February 2022, available at:

<http://www.tandfonline.com/10.1080/02640414.2022.2042146>.

Please refer to the original source for the final version of this work:

<https://doi.org/10.1080/02640414.2022.2042146>

Title: The validity of using Inertial Measurement Units to monitor the torso and pelvis sagittal plane motion of elite rowers.

Sara M. Brice^a, Emma L. Millett^{b,c}, and Bronson Philippa^d

^a*Physical Sciences, College of Science and Engineering, James Cook University, Townsville, Australia*

^b*Biomechanics, New South Wales Institute of Sport, Sydney, Australia*

^c*Athletics Australia, Melbourne, Australia*

^d*College of Science and Engineering, James Cook University, Cairns, Australia*

Orcid IDs

Sara M. Brice: 0000-0001-6766-4184

Bronson Philippa: 0000-0002-5736-0336

Twitter handles:

Sara M. Brice: @SarBrice

Corresponding author:

Sara M. Brice

James Cook University, Townsville, Australia, 4811.

Tel: +61 7 4781 4399

Fax: +61 7 4781 6788

Email: sara.brice1@jcu.edu.au

1 **Abstract**

2 In elite sport, inertial measurement units (IMUs) are being used increasingly to measure
3 movement in-field. IMU data commonly sought are body segment angles as this gives insights
4 into how technique can be altered to improve performance and reduce injury risk. The purpose
5 of this was to assess the validity of IMU use in rowing and identify if IMUs are capable of
6 detecting differences in sagittal torso and pelvis angles that result from changes in stroke rates.
7 Eight elite female rowers participated. Four IMUs were positioned along the torso and over the
8 pelvis of each athlete. Reflective markers surrounded each IMU which were used to compute
9 gold-standard data. Maxima, minima, angle range, and waveforms for ten strokes at rates of
10 20, 24, 28, and 32 strokes per minute were analysed. Root mean square errors as a percentage
11 of angle range fell between 1.44 and 8.43%. In most cases when significant differences ($p <$
12 0.05) in the angles were detected between stroke rates, this was observed in both IMU and
13 gold-standard angle data. These findings suggest IMUs are valid for measuring torso and pelvis
14 angles when rowing, and are capable of detecting differences that result from changes in stroke
15 rate.

16

17 **Keywords:** Rowing; Biomechanics; Engineering; Measurement

18

19 **Introduction**

20

21 Rowing is a demanding Olympic sport where success relies heavily on athletes moving in time
22 with one another, and on the coordinated inter-joint movement of each individual (Buckeridge
23 et al., 2015; Zainuddin et al., 2019). Performance is also reliant on the ability of each athlete to
24 transfer the force they generate at the foot stretcher to the oar which is then used to propel the
25 boat forward (Baudouin & Hawkins, 2002). The trunk plays an important role in the

26 transmission of foot stretcher forces to the oar, and in linking the lower and upper extremities
27 (Baudouin & Hawkins, 2002). For this reason, rowing spinal and pelvic kinematics and kinetics
28 has received a lot of research attention (Buckeridge et al., 2015, 2016; Martinez-Valdes et al.,
29 2019; McGregor et al., 2005; Trompeter et al., 2019; Wilson et al., 2013). A further reason for
30 the focus on spinal and pelvic motion in the literature is that the back is the most common site
31 of injury for elite rowers (Newlands et al., 2015; Smoljanovic et al., 2015; Trease et al., 2020).

32

33 Previous studies have found that rowers who suffer from low back pain exhibit greater pelvic
34 rotation and have less efficient trunk muscle activity (Martinez-Valdes et al., 2019; McGregor
35 et al., 2002; Nugent et al., 2021). Previous work has also found that as stroke rates increase
36 there are increases in back injury risk factors which is specifically exhibited by increases in the
37 shear and compressive forces in the lumbo-pelvic region (Buckeridge et al., 2016).
38 Furthermore, stroke rate increases have also been associated with increases in the range of
39 motion at the lumbo-pelvic, lumbar spine, and thoracic spine regions (Buckeridge et al., 2016;
40 Li et al., 2020; Wilson et al., 2013) which can all have implications for loading on the back.

41

42 Most of the aforementioned studies have examined rowing on ergometers primarily due to the
43 difficulties that surround measurement on-water. This is problematic as previous work has
44 found that on-water rowing movements are significantly different to movements performed on
45 an ergometer (Wilson et al., 2013). It would therefore be beneficial to athletes, coaches, and
46 practitioners if data surrounding spinal and pelvic movement could be accurately collected on-
47 water. One measurement device capable of this are portable electrogoniometers; however,
48 many of these systems require bulky data loggers to be worn. Another measurement device
49 being used increasingly to measure movements of athletes in-field are inertial measurement
50 units (IMUs). IMUs are lightweight, small in size, and do not require additional data loggers

51 to be worn. IMUs consist of accelerometers, gyroscopes, and magnetometers and the signals
52 from these sensors can be combined using fusion algorithms (Kalman, 1960; Madgwick et al.,
53 2011) to measure body segment motion.

54

55 Previous work has found that IMUs are valid for measuring segment motion and relative
56 segment motion in a number of movements and sporting disciplines (Bergamini et al., 2013;
57 Blair et al., 2018; Brice et al., 2018; Brice et al., 2020; Brouwer et al., 2020; Cottam et al.,
58 2018; Faber et al., 2009; Hindle et al., 2020; Liu et al., 2020). Concerning work that has
59 reported on the validity of IMUs for measuring sagittal plane relative angles, Brice et al. (2020)
60 examined the relative angle between the torso and pelvis and found root mean square errors
61 (RMSE) ranged between $2.9 \pm 1.3^\circ$ and $3.1 \pm 1.5^\circ$ depending on the IMU's location on the spine.
62 Concerning the work that has reported on the validity of IMUs for measuring sagittal plane
63 segment motion, Bergamini et al. (2013) examined trunk inclination during the running sprint
64 start and reported an RMSE of $3 \pm 3^\circ$ while Faber et al. (2009) reported an RMSE of $4.6 \pm 2.9^\circ$
65 when they investigated trunk inclination during a bent over lifting task. While numerous studies
66 have found IMUs to be valid, it is noted that the degree of accuracy is site and task specific
67 (Cuesta-Vargas et al., 2010) which is evident in the aforementioned studies. To our knowledge,
68 one previous study has investigated the validity of IMU use in rowing (King et al., 2009). The
69 findings of this study indicated that IMUs located over the pelvis and thoracolumbar (L1/T12)
70 juncture can validly measure sagittal plane inclination angles; however, novice rowers were
71 used in this study and stroke rate information was not reported. Given that novice rowers were
72 analysed it is possible that the stroke rates used by the rowers in this study were below what
73 elite rowers would commonly work at in training and competition. It is possible that as stroke
74 rates increase the error in the IMU angles may change due to the increased movement speed.
75 King et al. (2009) also investigated the impact of poor technique on IMU measured angles.

76 Visual inspection of the IMU waveforms was undertaken and differences were visible. Another
77 study that used IMUs to assess differences in technique is that of Klitgaard et al. (2021) who
78 examined the differences between elbow, shoulder, and knee angles when kayaking on-water
79 versus on an egometer. Statically significant differences were evident in the IMU data that were
80 collected for the two kayaking conditions. In both the aforementioned studies, there were no
81 comparisons made between the IMU data and a gold-standard to assess if the differences that
82 were evident in the IMU data were identical to that of a gold-standard. One previous study that
83 did compare IMU angles with a gold-standard found IMUs are capable of detecting technique
84 differences in shoulder and elbow flexion during canoeing (Liu et al., 2020). It would also be
85 desirable to know if IMUs have the precision to be able to detect the changes in the spinal
86 motion of rowers that are detected by gold-standard 3D motion capture systems.

87

88 The purpose of this present study was two-fold. The first aim was to assess the validity of the
89 IMeasureU (Oxford Metrics, Oxford, UK) IMUs for measuring sagittal plane motion of the
90 spine and pelvis when rowing at different stroke rates. The second aim was to examine if the
91 IMUs were capable of detecting if and when there were differences in the angle between stroke
92 rates.

93

94 **Materials and Methods**

95

96 Eight elite female rowers participated in this study which was given ethical approval by the
97 James Cook University Human Research Ethics Committee. All eight were national team
98 members and competing at an international level at the time of data collection. Prior to data
99 collection, all subjects gave written informed consent. A priori sample size calculation with an

100 alpha level of 0.05 found that seven participants was sufficient to generate statistical power of
101 80% with a large effect size.

102

103 Participants performed a self-selected warm-up and then rowed continuously for seven minutes
104 on an ergometer (Concept 2, Morrisville, VT, USA). Before rowing commenced each
105 participant sat in an upright stationary position on the ergometer. The angle of the spine relative
106 to the vertical in this position was then defined as zero degrees. Participants rowed for one
107 minute at rates of 20, 24, 28, and 32 strokes per minute. These stroke rates were chosen as they
108 are reflective of the rates used during the incremental “step test” which is commonly used to
109 monitor the training levels and fitness of rowers, and are reflective of a range of normal training
110 intensities (McGregor et al., 2005). Between each increment, participants rowed for one minute
111 at 18 strokes per minute for active recovery. Each participant had four IMeasureU IMUs v2.0
112 (Oxford Metrics, Oxford, UK) positioned on their back and pelvis. Each IMU consisted of tri-
113 axial accelerometers (± 16 g), gyroscopes (± 2000 °/s), and magnetometers (± 1200 mT). The
114 average maximum angular speed of the rowing motion measured in this study was 288 ± 62 °/s
115 which is well below the range specified by the manufacturers. IMUs were located over the
116 spinous processes of the first thoracic (T1 sensor), seventh thoracic (T7 sensor), second lumbar
117 (L2 sensor), and second sacral (S2 sensor) vertebrae. The T1, T7, and L2 sensors were mounted
118 on rigid plastic boards with three retro-reflective markers surrounding them. The S2 sensor was
119 skin mounted with three markers positioned around it. The S2 sensor and markers were not
120 placed on a plastic board as this part of the pelvis is flat. The markers were used to compute
121 the gold-standard angle data.

122

123 Throughout the seven minutes of rowing, IMU data was logged to an on-board SD card at
124 500Hz. The IMUs were used in accordance with the manufacturer’s instructions and were

125 operated and synchronised using the manufacturer's custom applications. When the
126 participants were rowing at stroke rates of 20, 24, 28, and 32 strokes per minute, marker
127 location data were also collected at 250Hz. Marker locations were collected using a 14 Vicon
128 Vantage camera system and the Vicon Nexus v2.8 software (Oxford Metrics, Oxford, UK). A
129 fifth IMU (sync IMU) was used during data collection to allow motion capture and IMU data
130 to be synchronized during post-processing. This involved aligning magnetic pulses from an
131 electromagnet that were collected by the analogue input of the motion capture system and the
132 sync IMU (Brice et al., 2020).

133

134 Marker data were filtered in Vicon Nexus using a Woltring filter with a mean standard error of
135 9 mm. This filter level was determined via a residual analysis (Winter, 2009). IMU data were
136 processed using custom Matlab scripts (Mathworks, Natic, USA). Firstly, the magnetometers
137 were calibrated using an ellipsoid fitting procedure. General descriptions of this procedure have
138 previously been reported (Gebre-Egziabher, 2007; Li & Li, 2012). However, in our
139 implementation, the fitting was constrained to find only ellipsoids whose principal axes align
140 with the IMU's axes, because we found that restricting the fitting in this way increased its
141 robustness when the magnetometer had not been fully rotated through all possible angles during
142 the data collection. These constrained ellipsoids correct for "hard iron" offsets in 3 axes, and
143 scale factor adjustments in 3 axes. The Kalman filter uses two reference vectors to define the
144 IMU orientation relative to a fixed laboratory reference frame. These two reference vectors are
145 the direction of gravity and the direction of the Earth's magnetic field. Gravity was taken to be
146 along the lab's Z axis. For the magnetic field reference, we extracted the magnetic field as
147 measured by each sensor during the initial part of each trial where the participants were
148 stationary on the ergometer. Each sensor measures the magnetic field in its own reference
149 frame, so we converted from the sensor's frame to the lab frame by rotating the measured

150 magnetic field using the orientation extracted from the Vicon system at the same moment in
151 time. The result was the Earth's magnetic field in the Vicon coordinate system according to
152 each of the IMUs. We then averaged over all sensors to give a single reference vector for the
153 direction of the magnetic field in the laboratory reference frame.

154

155 Since the parameter of interest was spinal flexion and extension, we extracted a scalar angle
156 from the 3D orientation of each sensor as shown in Figure 1. The angle of each sensor was
157 calculated as the angle between the lab Z axis and the sensor's Y axis, as indicated by the angle
158 θ in Figure 1. This angle was calculated using

$$159 \quad \theta = \text{atan} \frac{y_Y}{y_Z},$$

160 where y_Y and y_Z are the projection of the IMU y axis onto the lab Y and Z axes, respectively.
161 Angle calculations were performed separately for the Vicon data and the IMU data, resulting
162 in two different measurements of the same angle at every time step in the recording. Finally,
163 an anatomically neutral angle of 0° was defined as the position that each participant adopted
164 when they were seated stationary on the ergometer (see Table 1 for the mean angles of the
165 spine in this position). All angles are reported relative to this neutral position. It should be noted
166 that the sagittal plane angle calculated here is not calculated in the same manner as an
167 anatomical marker based model in a global reference frame. This has been noted previously in
168 the literature (Brice et al., 2020; Cottam et al. 2018).

169

170 [Figure 1 near here]

171 [Table 1 near here]

172

173 Ten complete strokes at the mid-point of the 20, 24, 28, and 32 stroke rate intervals were
174 selected for analysis. The maximum, minimum, and range of the sagittal plane inclination for

175 each stroke was determined for the four IMU locations. For each sensor location a total of 80
176 data points (eight athletes x ten strokes) for each discrete variable at each stroke rate were
177 examined. Discrete angle values were analysed as rowing literature that has examined spinal
178 motion has previously focused on examining discrete angle values. In addition to examining
179 discrete variables, the entire waveform for each participant's ten strokes at each stroke rate was
180 also examined. While waveforms of spinal angles have not been looked at in depth in the
181 literature, waveforms of other variables such as oar angle have been examined in rowing
182 (Warmenhoven et al., 2017). For the discrete variables, the root mean square error (RMSE)
183 and RMSE as a percentage of angle range (RMSE%) were determined, at each IMU location,
184 for each stroke rate (Bauer et al., 2015). 95% confidence intervals (CI_{Lower} and CI_{Upper}) were
185 also determined for RMSE. Bland-Altman biases and 95% limits of agreement (LOA_{Upper} and
186 LOA_{Lower}) were also computed (Bland & Altman, 1986). For each ten stroke waveform the
187 aforementioned comparison measures were determined. The comparison measures were then
188 averaged for each sensor for each of the stroke rates (Brice et al., 2020).

189

190 For each athlete, the average of the maximum angle, minimum angle, and angle range for each
191 stroke rate was determined for each sensor (i.e. average of the ten strokes examined). A
192 repeated measures ANOVA was then used to assess for a main effect of stroke rate for each
193 variable. The level of significance was set at $p < 0.05$. When significant main effects were
194 detected F values, p values, and effect sizes (partial η^2) were reported (Bakeman, 2005). The
195 effect sizes were classified as trivial (<0.0099), small ($0.0099 - 0.0587$), moderate ($0.0588 -$
196 0.1378), and large (≥ 0.1379) (Cohen, 1988). Where there were main effects detected, post-hoc
197 tests with a Bonferroni adjustment were used to identify where the differences were and
198 adjusted p values and effect sizes (Cohen's d) were reported. The adjusted effect sizes were
199 classified as trivial ($0 - 0.19$), small ($0.20 - 0.49$), moderate ($0.50 - 0.79$), and large (≥ 0.80)

200 (Cohen, 1988). This was done to assess if the IMUs were capable of identifying changes in the
201 maximum, minimum, and range of the angle between the stroke rates if they were present.

202

203 **Results**

204

205 There was strong agreement between the angles measured using the IMUs and the motion
206 capture system (Table 2a and 2b; Figure 2-5). Considering first the discrete values, RMSE
207 values ranged from between 1.05° and 4.90° with the average being $2.29 \pm 0.97^\circ$. RMSE%
208 values ranged from 1.44% to 8.43% with the average being $3.93 \pm 1.99\%$. Bland-Altman biases
209 ranged from -3.09° to 2.87° with the average being $1.31 \pm 0.21^\circ$. In most cases the biases were
210 positive which indicates the IMUs generally overestimated the maximum, minimum, and range
211 of the angle at each sensor location (Table 2a and 2b). Considering the waveforms, RMSE
212 values ranged from between 1.19° and 3.77° with the average being $2.16 \pm 0.93^\circ$. RMSE%
213 values ranged from 1.55% to 7.11% with the average being $3.79 \pm 2.24\%$. Bland-Altman biases
214 ranged from -0.91° to 1.51° with the average being $-0.02 \pm 0.72^\circ$. In most cases the biases were
215 negative which indicates that for the overall waveform the IMUs slightly underestimated the
216 angle at each sensor location.

217

218 [Table 2a near here]

219 [Table 2b near here]

220 [Figure 2 near here]

221 [Figure 3 near here]

222 [Figure 4 near here]

223 [Figure 5 near here]

224

225

226 Assessment of whether the IMUs were capable of identifying if and when stroke rate
227 significantly altered the maximum, minimum, and range of the angles revealed that the IMUs
228 had similar results to that of the gold-standard 3D motion capture system's measurements.
229 There were three instances for both gold-standard and IMU angles where main effects of stroke
230 rate were observed. A main effect was observed in the minima for T1 (gold-standard: $F = 6.861$,
231 $p = 0.026$, partial $\eta^2 = 0.533$ [large] and IMU: $F = 7.455$, $p = 0.017$, partial $\eta^2 = 0.554$ [large]),
232 in the minima for T7 (gold-standard: $F = 6.021$, $p = 0.005$, partial $\eta^2 = 0.501$ [large] and IMU:
233 $F = 3.614$, $p = 0.033$, partial $\eta^2 = 0.376$ [large]), and in the maxima for T7 (gold-standard: $F =$
234 21.211 , $p = 0.000$, partial $\eta^2 = 0.780$ [large] and IMU $F = 13.236$, $p = 0.000$, partial $\eta^2 = 0.688$
235 [large]). Where main effects were observed, post-hoc testing results revealed the following for
236 both the 3D motion capture angles and the IMU angles (Table 3):

- 237 - T1 minima were significantly greater for step 24 than steps 28 and 32
- 238 - T7 minima were significantly greater for step 24 than steps 28 and 32.
- 239 - T7 maxima were significantly smaller for step 20 than steps 28 and 32
- 240 - T7 maxima were significantly smaller for step 24 than step 32

241 There was one post-hoc testing result observed for 3D motion capture angles that was not
242 observed for the IMU angles which was that T7 maxima were significantly smaller for step 28
243 than step 32 (Table 3).

244 [Table 3 near here]

245

246 Discussion

247 The purpose of this investigation was two-fold. The first aim was to assess the validity of the
248 IMeasureU IMUs for measuring torso and pelvis sagittal plane inclination when rowing at
249 different stroke rates. Sagittal plane inclination at three torso locations (T1, T7, and L1) and

250 the pelvis (S2) for four different stroke rates (20, 24, 28, and 32 strokes per minute) was
251 measured. Ten strokes at each stroke rate for each athlete were examined. For each stroke the
252 angle's maximum, minimum, and range were determined. Discrete angle validity was assessed
253 by comparing maximum, minimum, and range for each stroke measured by the IMUs at each
254 location with angles measured by a 3D motion capture system (gold-standard). For the entire
255 ten strokes measured at each sensor location for each athlete, the waveforms were also
256 examined for all four stroke rates. Like the discrete variables, waveform validity was assessed
257 by comparing the ten stroke waveforms measured by the IMUs and the 3D motion capture
258 system waveforms at each sensor location. The second aim was to examine if the IMUs were
259 capable of identifying if and when stroke rate significantly altered the angles. This was assessed
260 by comparing the average of each athlete's maximum, minimum, and range at each sensor
261 location for each stroke rate.

262

263 Concerning the first aim, it has been reported that for a measurement system to be considered
264 valid RMSE% values should be below 10% (Walgaard et al., 2016) and RMSE values should
265 be below 5° (McGinley et al., 2009). All RMSE% and RMSE values were below these limits
266 (Table 2a and b) which indicates that the IMUs are valid for measuring sagittal plane trunk
267 inclination during rowing. The level of agreement that we observed is similar to what has been
268 observed by others who have also examined IMU use for measuring trunk inclination relative
269 to the vertical during sporting activities (Bergamini et al., 2013; King et al., 2009). The level
270 of agreement we observed is slightly lower than what has been observed with electromagnetic
271 devices (Bull & McGregor, 2000); however, these devices are constrained to the laboratory
272 environment which is a limitation that IMUs overcome. To our knowledge only one previous
273 study (King et al., 2009) has attempted to validate IMU use in rowing. In this previous study
274 novice rowers were examined and IMUs were located at the L1/T12 juncture and on the pelvis.

275 An average error of 3.98° was observed at L1/T12 while the error at the pelvis was slightly
276 higher at 4.08°. We also observed that the pelvis IMUs error was slightly higher (Table 2a and
277 2b). In the previous study they did not report the stroke rate of the novice rowers which was
278 noted in our introduction as a limiting factor. Novice rowers may not row at the rates expected
279 of elite athletes and differences in movement speed may impact on IMU validity. In our study
280 we addressed this by investigating a number of stroke rates and found that stroke rate did not
281 impact on the accuracy of the IMUs. This provides confidence to practitioners that IMUs are a
282 suitable device to use in the assessment and monitoring of torso and pelvis motion in training
283 and competition where varied stroke rates occur.

284

285 Concerning the second aim of our study, the IMUs and 3D motion capture system detected
286 identical main effects of stroke rate on the maxima at T7 and the minima at T1 and T7. Post-
287 hoc tests further revealed that all findings were identical with the exception being that for the
288 3D motion capture data the T7 maxima were significantly smaller for step 28 than step 32
289 (Table 3). It should be noted that while not significant, an identical trend was present for the
290 step 28 and 32 T7 IMU maxima (Table 3). These findings suggest that the IMUs examined in
291 this study are capable of detecting differences in technique; however, care should be taken
292 particularly when using an IMU located at T7. To our knowledge one previous study has
293 examined whether the IMU traces for different rowing techniques are different. King et al.
294 (2009) provided novice rowers with examples of good technique and two types of bad
295 technique. The participants were then instructed to row with the three techniques they had been
296 shown. Angle traces from IMUs located at the L1/T12 juncture and over the pelvis were
297 compared to see if visual differences were present in the waveforms. Visually the waveforms
298 looked different (predominantly at the maxima); however, there was no comparison with gold-
299 standard angles and the waveforms of single participant were presented. Despite this King et

300 al. (2009) claim that the IMUs were capable of identifying differences in technique which our
301 statistical analysis supports.

302

303 It should be noted that our study had some limiting factors. First, a small number of athletes
304 were used. Care should be taken particularly when drawing conclusions from our between
305 stroke rate comparisons of the angles we measured. It is also possible that the errors we
306 observed may have been different had a larger sample been examined, although nearly all 95%
307 confidence interval upper limits were below values reported as being acceptable in the
308 literature. Second, we carried out our validation on an ergometer. It should be noted that the
309 error in the IMU angles may be different when rowing on-water and future work should attempt
310 to validate IMU use on-water to assess if the error is significantly different to what is observed
311 on an ergometer. Third, while we did examine stroke rates that are reflective of the different
312 training intensities (McGregor et al., 2005), others have found even higher stroke rates can be
313 used in competition (Silva et al., 2020). For all stroke rates we investigated we did find that the
314 IMUs were valid and future work should consider confirming that the IMUs continue to be
315 valid when using higher stroke rates.

316

317 **Conclusion**

318

319 This study investigated the accuracy of sagittal plane torso and pelvis angle data collected using
320 IMUs when rowing at four different stroke rates. The angles measured by the IMUs were found
321 to be highly valid as there was close agreement between IMU angles and those measured using
322 the gold-standard 3D motion capture system. We also investigated whether the IMUs were
323 capable of detecting if and when differences in stroke rate altered the sagittal plane angles. We
324 found that in most instances significant differences detected in the gold-standard angles were

325 also detected in the IMU angles. Our work suggests that IMUs are a viable option for measuring
326 accurate sagittal plane angle data during rowing.

327

328 **Acknowledgements:**

329 The authors wish to thank the New South Wales Institute of Sport staff for their assistance with
330 the data collection and for provision of the equipment for this data collection.

331

332 **Declaration of interest statement:**

333 The authors report no conflict of interest.

334

335 **References**

336 Bakeman, R. (2005). Recommended effect size statistics for repeated measures designs.

337 *Behavior research methods*, 37(3), 379-384. <https://doi.org/10.3758/BF03192707>

338

339 Baudouin, A., & Hawkins, D. (2002). A biomechanical review of factors affecting rowing
340 performance. *British Journal of Sports Medicine*, 36(6), 396-402.

341 <https://doi.org/10.1136/bjism.36.6.396>

342

343 Bauer, C. M., Rast, F. M., Ernst, M. J., Kool, J., Oetiker, S., Rissanen, S. M., Suni, J. H., &

344 Kankaanpää, M. (2015). Concurrent validity and reliability of a novel wireless inertial

345 measurement system to assess trunk movement. *Journal of Electromyography and*

346 *Kinesiology*, 25(5), 782-790. <https://doi.org/http://dx.doi.org/10.1016/j.jelekin.2015.06.001>

347

348 Bergamini, E., Guillon, P., Camomilla, V., Pillet, H., Skalli, W., & Cappozzo, A. (2013). Trunk
349 inclination estimate during the sprint start using an inertial measurement unit: A Validation
350 Study. *Journal of Applied Biomechanics*, 29(5), 622-627. <https://doi.org/10.1123/jab.29.5.622>
351

352 Blair, S., Duthie, G., Robertson, S., Hopkins, W., & Ball, K. (2018). Concurrent validation of
353 an inertial measurement system to quantify kicking biomechanics in four football codes.
354 *Journal of Biomechanics*, 73, 24-32.
355 <https://doi.org/https://doi.org/10.1016/j.jbiomech.2018.03.031>
356

357 Bland, J. M., & Altman, D. G. (1986). Statistical methods for assessing agreement between
358 two methods of clinical measurement. *Lancet*, 1. 307-310 [https://doi.org/10.1016/s0140-](https://doi.org/10.1016/s0140-6736(86)90837-8)
359 [6736\(86\)90837-8](https://doi.org/10.1016/s0140-6736(86)90837-8)
360

361 Brice, S. M., Hurley, M., & Phillips, E. J. (2018). Use of inertial measurement units for
362 measuring torso and pelvis orientation, and shoulder–pelvis separation angle in the discus
363 throw. *International Journal of Sports Science & Coaching*, 13(6), 985-992.
364 <https://doi.org/10.1177/1747954118778664>
365

366 Brice, S. M., Phillips, E. J., Millett, E. L., Hunter, A., & Philippa, B. (2020). Comparing inertial
367 measurement units and marker-based biomechanical models during dynamic rotation of the
368 torso. *European Journal of Sport Science*, 20(6), 767-775.
369 <https://doi.org/10.1080/17461391.2019.1666167>
370

371 Brouwer, N., Yeung, T., Bobbert, M., & Besier, T. (2020). 3D trunk orientation measured using
372 inertial measurement units during anatomical and dynamic sports motions. *Scandinavian*
373 *Journal of Medicine & Science in Sports*, 31(2), 1-13. <https://doi.org/10.1111/sms.13851>
374

375 Buckeridge, E. M., Bull, A. M. J., & McGregor, A. H. (2015). Biomechanical determinants of
376 elite rowing technique and performance. *Scandinavian Journal of Medicine & Science in*
377 *Sports*, 25(2), e176-e183. <https://doi.org/10.1111/sms.12264>
378

379 Buckeridge, E. M., Bull, A. M. J., & McGregor, A. H. (2016). Incremental training intensities
380 increases loads on the lower back of elite female rowers. *Journal of Sports Sciences*, 34(4),
381 369-378. <https://doi.org/10.1080/02640414.2015.1056821>
382

383 Bull, A. M. J., & McGregor, A. H. (2000). Measuring spinal motion in rowers: the use of an
384 electromagnetic device. *Clinical biomechanics*, 15(10), 772-776.
385 [https://doi.org/10.1016/S0268-0033\(00\)00043-7](https://doi.org/10.1016/S0268-0033(00)00043-7)
386

387 Cohen, J. (1988). *Statistical power analysis for the behavioral sciences* (2nd ed.). Lawrence
388 Erlbaum Associates.
389

390 Cottam, D., Kosovich, S., Campbell, A., Davey, P., Kent, P., Tan, J.-S., Elliott, B., & Alderson,
391 J. (2018, September). Can inertial measurement units be used to measure pelvis and thorax
392 motion during cricket. In P. Hume, J. Alderson, & B. Wilson (Eds.), *Proceedings of the 36th*
393 *International Conference of Biomechanics in Sports* (pp 350-353). International Society of
394 Biomechanics in Sport. Retrieved from <https://commons.nmu.edu/isbs/vol36/iss1/66/>
395

396 Cuesta-Vargas, A. I., Galán-Mercant, A., & Williams, J. M. (2010). The use of inertial sensors
397 system for human motion analysis. *Physical Therapy Reviews*, 15(6), 462-473.
398 <https://doi.org/10.1179/1743288X11Y.0000000006>

399

400 Faber, G. S., Kingma, I., Bruijn, S. M., & van Dieën, J. H. (2009). Optimal inertial sensor
401 location for ambulatory measurement of trunk inclination. *Journal of Biomechanics*, 42(14),
402 2406-2409. <https://doi.org/https://doi.org/10.1016/j.jbiomech.2009.06.024>

403

404 Gebre-Egziabher, D. (2007). Magnetometer Autocalibration Leveraging Measurement Locus
405 Constraints. *Journal of Aircraft*, 44(4), 1361-1368. <https://doi.org/10.2514/1.27118>

406

407 Hindle, B. R., Keogh, J. W. L., & Lorimer, A. V. (2020). Validation of Spatiotemporal and
408 Kinematic Measures in Functional Exercises Using a Minimal Modeling Inertial Sensor
409 Methodology. *Sensors*, 20(16), Article 4586. <https://www.mdpi.com/1424-8220/20/16/4586>

410

411 Kalman, R. E. (1960). A New Approach to Linear Filtering and Prediction Problems. *Journal*
412 *of Basic Engineering*, 82(1), 35-45. <https://doi.org/10.1115/1.3662552>

413

414 King, R. C., McIlwraith, D. G., Lo, B., Pansiot, J., McGregor, A. H., & Yang, G. (2009, June).
415 Body Sensor Networks for Monitoring Rowing Technique. In P.K Wright, & E.M.Yeatman
416 (Eds.) *Proceedings of the 6th International Workshop on Wearable and Implantable Body*
417 *Sensor Networks* (pp. 251-255). Institute of Electrical and Electronics Engineers. Retrieved
418 from [https://doi: 10.1109/BSN.2009.60](https://doi:10.1109/BSN.2009.60)

419

420 Klitgaard, K. K., Hauge, C., Oliveira, A. S., & Heinen, F. (2021). A kinematic comparison of
421 on-ergometer and on-water kayaking. *European Journal of Sport Science*, 21(10), 1375-1304.
422 <https://doi.org/10.1080/17461391.2020.1831617>
423

424 Li, Y., Koldenhoven, R. M., Jiwan, N. C., Zhan, J., & Liu, T. (2020). Trunk and shoulder
425 kinematics of rowing displayed by Olympic athletes. *Sports Biomechanics*. Advance online
426 publication. <https://doi.org/10.1080/14763141.2020.1781238>
427

428 Li, X., & Li, Z. (2012). A new calibration method for tri-axial field sensors in strap-down
429 navigation systems. *Measurement Science and Technology*, 23(10), 105105.
430 <https://doi.org/10.1088/0957-0233/23/10/105105>
431

432 Liu, L., Qiu, S., Wang, Z., Li, J., & Wang, J. (2020). Canoeing Motion Tracking and Analysis
433 via Multi-Sensors Fusion. *Sensors*, 20(7), 2110. <https://doi.org/10.3390/s20072110>
434

435 Madgwick, S. O. H., Harrison, A. J. L., & Vaidyanathan, R. (2011, June-July). Estimation of
436 IMU and MARG orientation using a gradient descent algorithm. In R. Gassert, J. Herder, S.
437 Micera, R. Riener, & P. Wolf (Eds.), *Proceedings of the 2011 IEEE International Conference*
438 *on Rehabilitation Robotics* (pp. 1-7). Institute of Electrical and Electronics Engineers.
439 Retrieved from [https://doi: 10.1109/ICORR.2011.5975346](https://doi:10.1109/ICORR.2011.5975346).
440

441 Martinez-Valdes, E., Wilson, F., Fleming, N., McDonnell, S.-J., Horgan, A., & Falla, D.
442 (2019). Rowers with a recent history of low back pain engage different regions of the lumbar
443 erector spinae during rowing. *Journal of Science and Medicine in Sport*, 22(11), 1206-1212.
444 <https://doi.org/http://dx.doi.org/10.1016/j.jsams.2019.07.007>

445

446 McGinley, J. L., Baker, R., Wolfe, R., & Morris, M. E. (2009). The reliability of three-
447 dimensional kinematic gait measurements: a systematic review. *Gait Posture*, *29*(3), 360–369.
448 <https://doi.org/10.1016/j.gaitpost.2008.09.003>

449

450 McGregor, A. H., Anderton, L., & Gedroyc, W. M. W. (2002). The trunk muscles of elite
451 oarsmen. *British Journal of Sports Medicine*, *36*(3), 214-217.
452 <https://doi.org/10.1136/bjism.36.3.214>

453

454 McGregor, A. H., Patankar, Z. S., & Bull, A. M. J. (2005). Spinal kinematics in elite
455 oarswomen during a routine physiological "step test". *Medicine and Science in Sports and*
456 *Exercise*, *37*(6), 1014-1020. <https://doi.org/10.1249/01.mss.0000171618.22263.58>

457

458 Newlands, C., Reid, D., & Parmar, P. (2015). The prevalence, incidence and severity of low
459 back pain among international-level rowers. *British Journal of Sports Medicine*, *49*(14), 951-
460 956. <https://doi.org/10.1136/bjsports-2014-093889>

461

462 Nugent, F. J., Vinther, A., McGregor, A., Thornton, J. S., Wilkie, K., & Wilson, F. (2021). The
463 relationship between rowing-related low back pain and rowing biomechanics: a systematic
464 review. *British Journal of Sports Medicine*. *55*(11), 616-630. [https://doi.org/10.1136/bjsports-](https://doi.org/10.1136/bjsports-2020-102533)
465 [2020-102533](https://doi.org/10.1136/bjsports-2020-102533)

466

467 Silva, F. B. M. d., Brito, J. P. R. G. M. d., & Gomes, A. C. (2020). Olympic rowing: model of
468 competitive activity of international level elite female athletes. *Revista brasileira de medicina*
469 *do esporte*, *26*(2), 162-166. <https://doi.org/10.1590/1517-869220202602218337>

470

471 Smoljanovic, T., Bohacek, I., Hannafin, J. A., Terborg, O., Hren, D., Pecina, M., & Bojanic, I.
472 (2015). Acute and chronic injuries among senior international rowers: a cross-sectional study.
473 *International Orthopaedics*, 39(8), 1623-1630. <https://doi.org/10.1007/s00264-014-2665-7>

474

475 Trease, L., Wilkie, K., Lovell, G., Drew, M., & Hooper, I. (2020). Epidemiology of injury and
476 illness in 153 Australian international-level rowers over eight international seasons. *British*
477 *Journal of Sports Medicine*, 54(21), 1288-1293. <https://doi.org/10.1136/bjsports-2019-101402>

478

479 Trompeter, K., Weerts, J., Fett, D., Firouzabadi, A., Heinrich, K., Schmidt, H., Brüggemann,
480 G.-P., & Platen, P. (2019). Spinal and Pelvic Kinematics During Prolonged Rowing on an
481 Ergometer vs. Indoor Tank Rowing. *Journal of Strength and Conditioning Research*. 35(9),
482 2622-2628. <https://doi.org/10.1519/JSC.00000000000003187>

483

484 Walgaard, S., Faber, G. S., van Lummel, R. C., van Dieën, J. H., & Kingma, I. (2016). The
485 validity of assessing temporal events, sub-phases and trunk kinematics of the sit-to-walk
486 movement in older adults using a single inertial sensor. *Journal of Biomechanics*, 49(9), 1933-
487 1937. <https://doi.org/http://dx.doi.org/10.1016/j.jbiomech.2016.03.010>

488

489 Wilson, F., Gissane, C., Gormley, J., & Simms, C. (2013). Sagittal plane motion of the lumbar
490 spine during ergometer and single scull rowing. *Sports Biomechanics*, 12(2), 132-142.
491 <https://doi.org/10.1080/14763141.2012.726640>

492

493 Winter, D. A. (2009). *Biomechanics and motor control of human movement* (4th ed.). John
494 Wiley & Sons, Inc.

495

496 Warmenhoven, J., Copley, S., Draper, C., Harrison, A. J., Bargary, N., & Smith, R. (2017).
497 Assessment of propulsive pin force and oar angle time-series using functional data analysis in
498 on-water rowing. *Scandinavian Journal of Medicine & Science in Sports*, 27(12), 1688-1696.
499 <https://doi.org/10.1111/sms.12871>

500

501 Zainuddin, F. L., Zahiran, A., Umar, M. A., Shahrudin, S., & Razman, R. M. (2019). Changes
502 in lower limb kinematics coordination during 2000m ergometer rowing among male junior
503 national rowers. *Journal of Physical Education and Sport*, 19(3), 1656-1662.
504 <https://doi.org/http://dx.doi.org/10.7752/jpes.2019.03240>

Table 1. Mean angle of the spine relative to the vertical for the participants while seated on the ergometer measured by the IMUs and by the 3D motion capture system (gold-standard data - GS). For the rowing trials, the spine was defined as being in 0° in this position. Standard deviations are indicated in brackets.

	Location			
	T1	T7	L1	S2
GS angle (°)	34.55 (6.43)	12.20 (9.25)	-5.38 (9.96)	-13.95 (8.41)
IMU angle (°)	34.96 (6.19)	10.53 (10.30)	-5.86 (11.82)	-12.09 (3.52)

Table 2a: Comparison between maximum, minimum, range, and waveforms of the angles measured by the IMUs and by the 3D motion capture system (gold-standard data) for stroke rates 20 and 24. Standard deviations are indicated in brackets for the waveform values.

		Rate 20				Rate 24			
		T1	T7	L1	S2	T1	T7	L1	S2
Max	RMSE (°)	1.88	1.55	1.23	3.74	2.21	1.71	1.37	4.12
	RMSE CI _{Lower} (°)	1.63	1.34	1.07	3.24	1.91	1.48	1.19	3.57
	RMSE CI _{Upper} (°)	2.22	1.83	1.46	4.42	2.61	2.02	1.62	4.87
	RMSE%	4.34	1.98	1.70	6.48	5.15	2.13	1.82	7.09
	Bias (°)	-1.05	0.94	0.49	-2.30	-0.85	0.89	0.68	-3.09
	LOA _{Upper} (°)	2.02	3.36	2.72	3.54	3.17	3.77	3.03	2.31
	LOA _{Lower} (°)	-4.13	-1.48	-1.74	-8.15	-4.88	-1.99	-1.67	-8.48
Min	RMSE (°)	1.75	1.73	1.05	3.72	1.77	1.85	1.11	3.68
	RMSE CI _{Lower} (°)	1.52	1.50	0.91	3.22	1.53	1.60	0.96	3.19
	RMSE CI _{Upper} (°)	2.07	2.05	1.24	4.40	2.09	2.18	1.31	4.35
	RMSE%	4.04	2.22	1.44	6.44	4.12	2.30	1.47	6.33
	Bias (°)	0.97	0.15	0.34	2.85	0.93	0.21	0.32	0.21
	LOA _{Upper} (°)	3.84	3.56	2.30	7.57	3.89	3.83	-1.77	7.53
	LOA _{Lower} (°)	-1.89	-3.26	-1.62	-1.87	-2.03	-3.41	2.41	-7.12
Range	RMSE (°)	1.63	2.07	1.71	3.38	1.52	2.29	1.79	4.90
	RMSE CI _{Lower} (°)	1.41	1.79	1.48	2.92	1.31	1.98	1.55	4.24
	RMSE CI _{Upper} (°)	1.93	2.44	2.02	3.99	1.80	2.71	2.12	5.79
	RMSE%	3.77	2.65	2.35	5.85	3.54	2.85	2.37	8.43
	Bias (°)	-0.08	1.09	0.83	0.55	0.08	1.10	1.00	-2.88
	LOA _{Upper} (°)	3.14	4.55	3.77	7.18	3.07	5.06	3.93	0.02
	LOA _{Lower} (°)	-3.29	-2.37	-2.11	-6.09	-2.92	-2.87	-1.93	-5.78
Waveform	RMSE (°)	1.85 (0.87)	1.26 (0.37)	1.19 (0.57)	3.77 (0.50)	2.05 (0.94)	1.31 (0.38)	2.05 (0.94)	3.63 (0.81)
	RMSE CI _{Lower} (°)	1.82 (0.85)	1.24 (0.36)	1.18 (0.56)	3.71 (0.49)	2.02 (0.92)	1.29 (0.38)	1.39 (0.81)	3.56 (0.79)
	RMSE CI _{Upper} (°)	1.88 (0.88)	1.28 (0.37)	1.21 (0.56)	3.83 (0.50)	2.09 (0.95)	1.34 (0.39)	1.44 (0.84)	3.69 (0.82)
	RMSE%	3.99 (2.21)	1.51 (0.41)	4.33 (1.26)	7.11 (0.64)	4.45 (1.47)	1.57 (0.43)	4.45 (1.47)	6.83 (1.75)
	Bias (°)	-0.82 (1.14)	0.16 (0.35)	-0.23 (0.71)	0.94 (1.90)	-0.79 (1.38)	0.00 (0.50)	-0.06 (0.60)	1.19 (0.97)
	LOA _{Lower} (°)	-3.56 (1.65)	-2.19 (0.85)	-2.23 (1.34)	-5.49 (2.34)	-3.75 (1.52)	-2.41 (0.88)	-2.60 (1.94)	-5.30 (1.90)
	LOA _{Upper} (°)	1.91 (1.65)	2.51 (0.81)	1.76 (0.88)	7.36 (1.55)	2.17 (2.32)	2.41 (0.95)	2.48 (1.46)	7.68 (1.99)

Table 2b: Comparison between maximum, minimum, range, and waveforms of the angles measured by the IMUs and by the 3D motion capture system (gold-standard data) for stroke rates 28 and 32. Standard deviations are indicated in brackets for the waveform values.

		Rate 28				Rate 32			
		T1	T7	L1	S2	T1	T7	L1	S2
Max	RMSE (°)	2.01	1.84	1.47	2.58	2.64	2.24	1.22	4.22
	RMSE CI _{Lower} (°)	1.74	1.59	1.30	2.23	2.28	1.94	1.06	3.66
	RMSE CI _{Upper} (°)	2.38	2.17	1.74	3.05	3.11	2.66	1.45	4.99
	RMSE%	4.92	2.32	1.97	4.65	6.78	2.84	1.65	7.33
	Bias (°)	0.05	1.05	0.62	-2.70	-0.26	0.55	0.39	-2.62
	LOA _{Upper} (°)	4.02	4.03	3.26	1.17	4.92	4.85	2.68	3.94
	LOA _{Lower} (°)	-3.91	-1.93	-2.03	-6.57	-5.44	-3.75	-1.89	-9.18
Min	RMSE (°)	1.72	1.92	1.34	4.00	2.66	2.32	1.58	3.14
	RMSE CI _{Lower} (°)	1.49	1.67	1.16	3.47	2.31	2.01	1.37	2.72
	RMSE CI _{Upper} (°)	2.04	2.27	1.58	4.74	3.15	2.75	1.87	3.71
	RMSE%	4.22	2.43	1.79	7.22	6.86	2.94	2.14	5.45
	Bias (°)	0.77	0.42	0.29	-0.09	0.74	0.59	0.46	2.87
	LOA _{Upper} (°)	3.81	4.12	2.87	7.86	5.77	5.02	3.44	5.85
	LOA _{Lower} (°)	-2.27	-3.28	-2.29	-8.04	-4.30	-3.85	-2.53	-0.11
Range	RMSE (°)	1.99	2.30	1.97	4.38	1.36	2.94	1.76	2.43
	RMSE CI _{Lower} (°)	1.71	1.99	1.70	3.79	1.18	2.54	1.53	2.10
	RMSE CI _{Upper} (°)	2.35	2.72	2.33	5.18	1.61	3.47	2.08	2.87
	RMSE%	4.87	2.90	2.63	7.89	3.51	3.72	2.39	4.22
	Bias (°)	0.82	1.47	0.91	-2.79	0.69	1.14	0.85	0.25
	LOA _{Upper} (°)	4.40	4.95	4.36	5.89	3.07	6.48	3.90	3.84
	LOA _{Lower} (°)	-2.75	-2.02	-2.54	-11.47	-1.69	-4.21	-2.20	-3.33
Waveform	RMSE (°)	2.44 (1.19)	1.76 (0.59)	1.47 (0.78)	3.14 (1.06)	2.45 (1.00)	1.72 (0.57)	1.31 (0.39)	3.73 (1.47)
	RMSE CI _{Lower} (°)	2.40 (1.17)	1.73 (0.58)	1.44 (0.77)	3.08 (1.04)	2.40 (0.98)	1.67 (0.56)	1.28 (0.38)	3.66 (1.44)
	RMSE CI _{Upper} (°)	2.49 (1.21)	1.80 (0.60)	1.49 (0.80)	3.20 (1.08)	2.50 (1.02)	1.75 (0.58)	1.34 (0.40)	3.81 (1.50)
	RMSE%	5.48 (2.94)	2.12 (0.68)	1.84 (0.87)	6.02 (2.31)	5.61 (2.62)	2.05 (0.62)	1.66 (0.43)	7.01 (2.71)
	Bias (°)	-0.91 (1.60)	-0.03 (0.53)	-0.16 (0.79)	0.32 (0.73)	-0.85 (1.15)	-0.24 (0.46)	-0.28 (0.82)	1.51 (1.76)
	LOA _{Lower} (°)	-4.43 (1.95)	-3.32 (1.35)	-2.68 (2.03)	-5.68 (1.70)	-4.82 (1.99)	-3.48 (1.11)	-2.38 (1.17)	-4.73 (1.42)
	LOA _{Upper} (°)	2.61 (3.13)	3.26 (1.38)	2.37 (1.13)	6.32 (2.57)	3.11 (2.57)	3.01 (1.22)	1.82 (0.59)	7.75 (3.57)

Table 3. Means of the maximum, minimum, and range of the gold-standard (GS) and IMU angles at each stroke rate for all eight participants.

Standard deviations are indicated in brackets.

Location	Step	Max GS (°)	Max IMU (°)	Min GS (°)	Min IMU (°)	Range GS (°)	Range IMU (°)
T1	20	14.28 (6.71)	13.23 (7.54)	-28.98 (10.26)	-29.96 (10.03)	43.26 (6.62)	43.18 (6.89)
	24	13.12 (7.45)	12.27 (7.32)	-29.76 (10.32) ^{AB}	-30.69 (9.92) ^{AB}	42.89 (6.98)	42.96 (7.50)
	28	12.87 (7.37)	12.93 (7.04)	-27.92 (10.47) ^A	-28.68 (10.24) ^A	40.79 (7.39)	41.61 (7.62)
	32	13.21 (7.30)	12.70 (7.29)	-25.63 (10.39) ^B	-26.83 (12.04) ^B	38.84 (10.08)	39.53 (9.88)
T7	20	38.61 (7.51) ^{CD}	39.56 (8.31) ^{CD}	-39.37 (8.94)	-39.52 (10.15)	77.98 (9.12)	79.08 (10.01)
	24	40.43 (6.65) ^E	41.32 (7.53) ^E	-39.87 (9.91) ^{GH}	-40.08 (10.92) ^{GH}	80.31 (9.27)	81.40 (10.07)
	28	41.50 (6.33) ^{CF}	42.55 (7.48) ^C	-37.62 (10.82) ^G	-38.04 (12.31) ^G	79.13 (9.22)	80.59 (10.12)
	32	42.92 (6.15) ^{DEF}	43.47 (7.56) ^{DE}	-36.02 (11.63) ^H	-36.60 (13.13) ^H	78.94 (10.57)	80.07 (11.63)
L1	20	36.88 (6.79)	37.38 (7.25)	-35.81 (8.00)	-36.15 (7.86)	72.70 (7.97)	73.53 (8.63)
	24	37.89 (5.82)	38.57 (5.95)	-37.59 (9.15)	-37.91 (8.99)	75.48 (8.12)	76.48 (8.48)
	28	38.63 (5.01)	39.24 (5.11)	-36.12 (9.54)	-36.41 (9.61)	74.74 (7.58)	75.65 (8.03)
	32	39.32 (4.54)	39.71 (4.38)	-34.53 (10.77)	-34.99 (10.66)	73.85 (9.03)	74.70 (9.46)
S2	20	28.07 (8.25)	25.23 (6.53)	-29.67 (9.30)	-27.42 (12.07)	57.74 (12.53)	52.65 (17.10)
	24	26.80 (6.98)	24.22 (6.62)	-31.31 (8.69)	-29.91 (13.52)	58.11 (11.96)	54.14 (18.88)
	28	25.38 (6.19)	22.41 (6.91)	-30.10 (6.97)	-29.84 (10.22)	55.48 (9.26)	52.25 (15.75)
	32	27.42 (8.81)	25.88 (13.93)	-30.18 (7.46)	-27.73 (12.55)	57.60 (11.72)	53.61 (19.42)

^AT1 Step 24 minima are significantly greater than Step 28 minima for GS ($p = 0.002$, $d = 2.01$ [large]) and IMU ($p = 0.001$, $d = 2.37$ [large])

^BT1 Step 24 minima are significantly greater than Step 32 minima for GS ($p = 0.009$, $d = 1.45$ [large]) and IMU ($p = 0.009$, $d = 1.44$ [large])

^CT7 Step 20 maxima are significantly smaller than Step 28 maxima for GS ($p = 0.036$, $d = 1.57$ [large]) and IMU ($p = 0.046$, $d = 1.49$ [large])

^DT7 Step 20 maxima are significantly smaller than Step 32 maxima for GS ($p = 0.008$, $d = 2.13$ [large]) and IMU ($p = 0.035$, $d = 1.58$ [large])

^ET7 Step 24 maxima are significantly smaller than Step 32 maxima for GS ($p = 0.004$, $d = 2.41$ [large]) and IMU ($p = 0.043$, $d = 1.51$ [large])

^FT7 Step 28 maxima are significantly smaller than Step 32 maxima for GS ($p = 0.041$, $d = 1.52$ [large])

^GT7 Step 24 minima are significantly greater than Step 28 minima for GS ($p = 0.03$, $d = 1.63$ [large]) and IMU ($p = 0.038$, $d = 1.00$ [large])

^HT7 Step 24 minima are significantly greater than Step 32 minima for GS ($p = 0.017$, $d = 1.83$ [large]) and IMU ($p = 0.013$, $d = 1.31$ [large])

Figure 1:

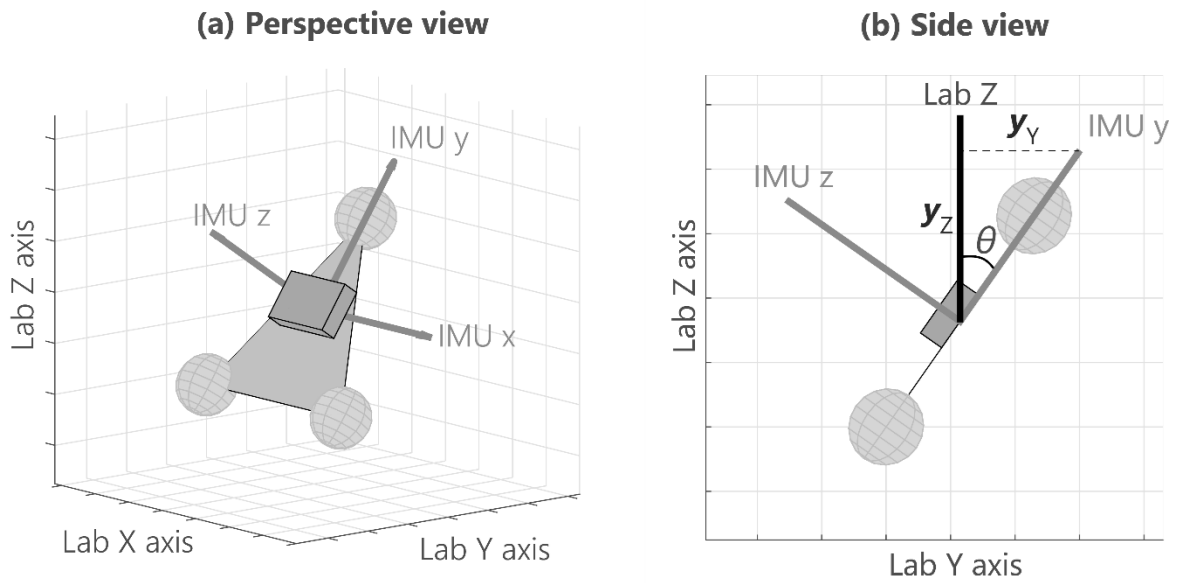


Figure 2:

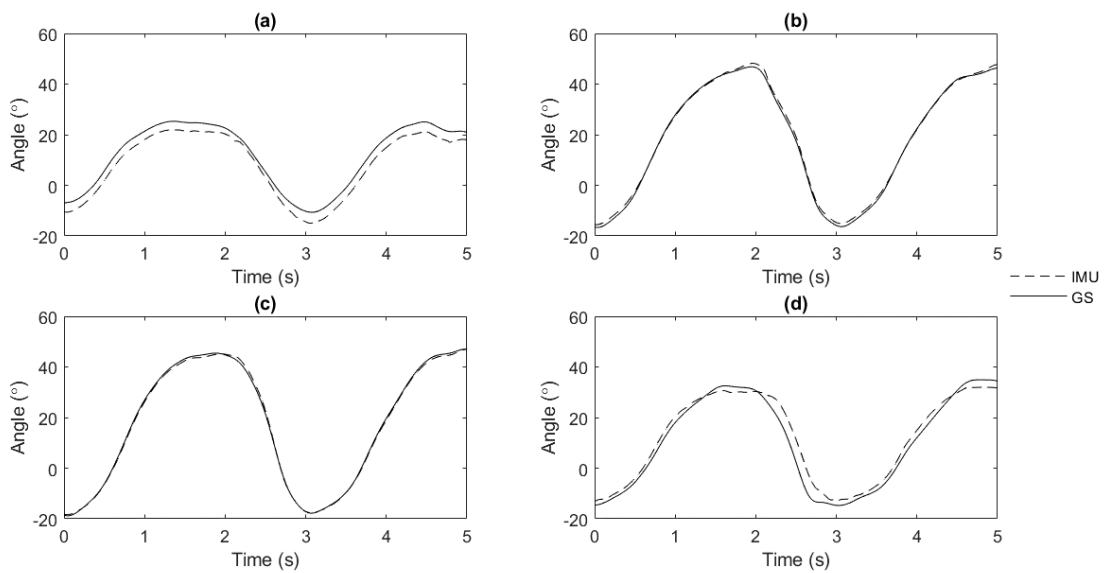


Figure 3:

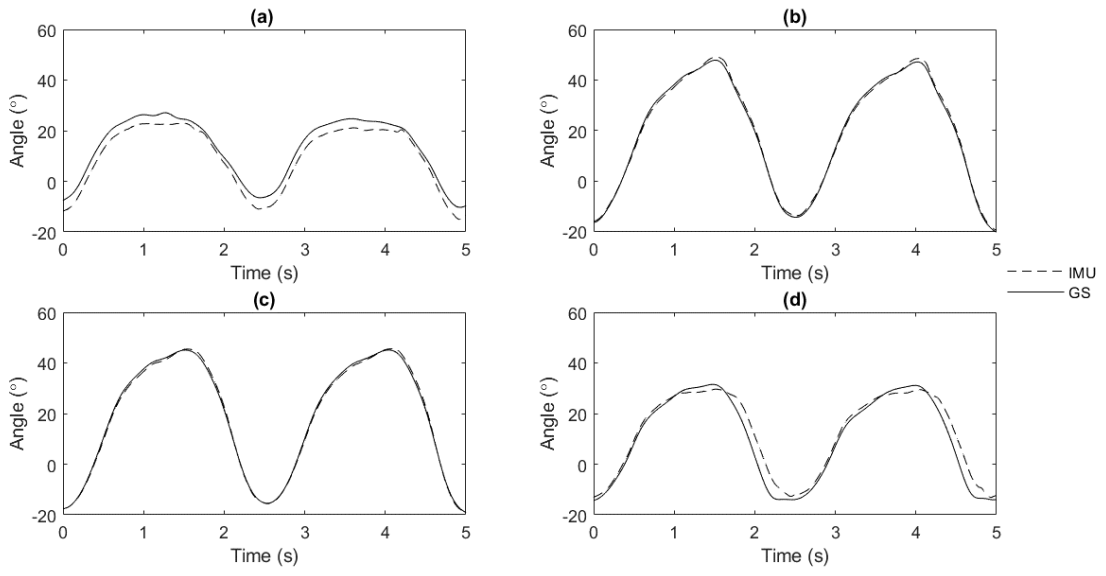


Figure 4:

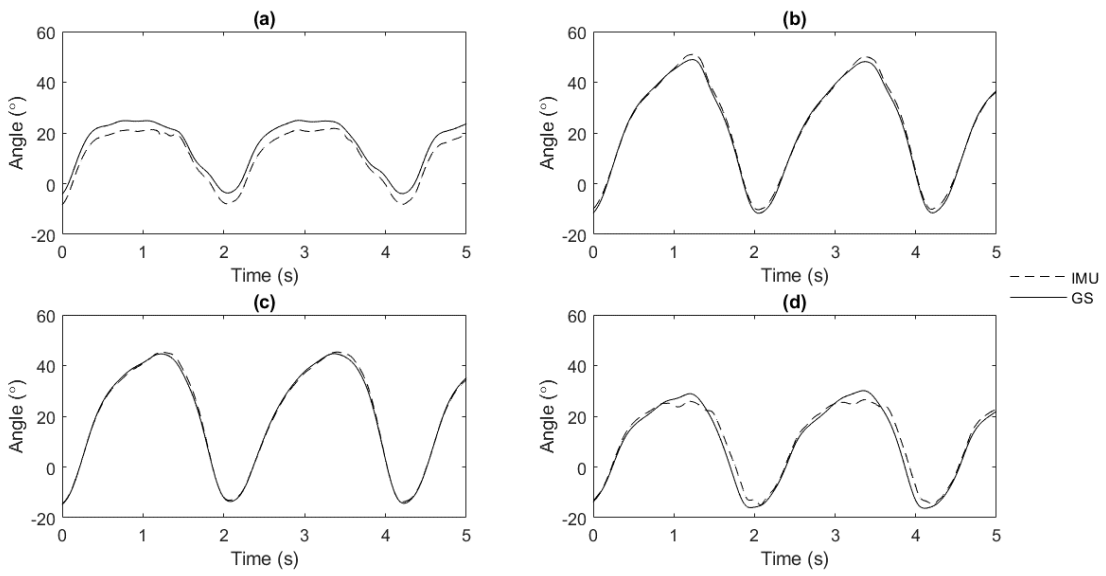


Figure 5:

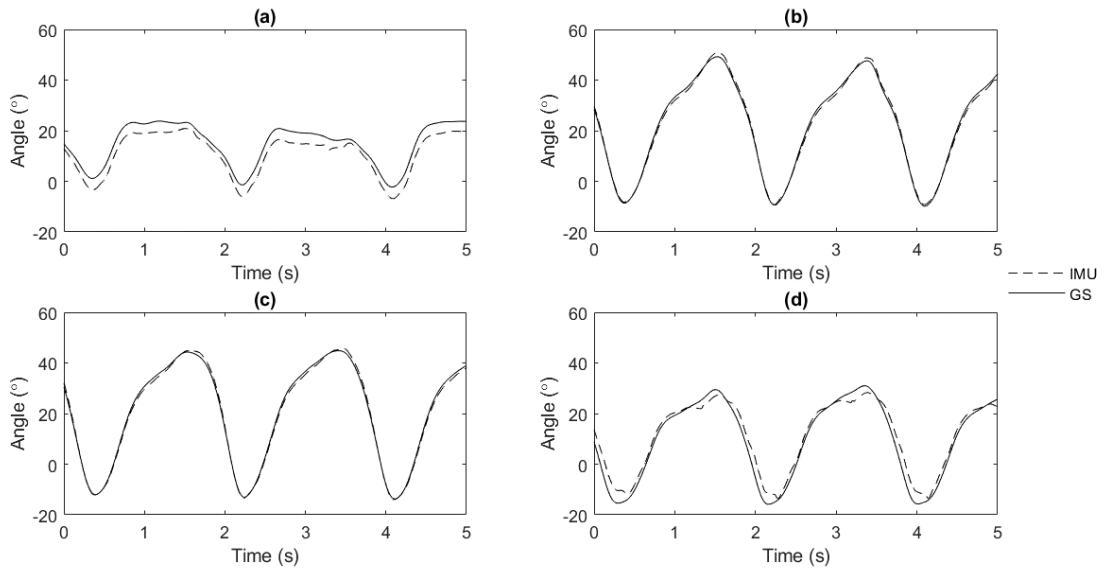


Figure captions:

Figure 1: Coordinate system used to analyse the orientation data, shown here in (a) 3D perspective and (b) the side view. The retro-reflective markers (grey circles) define the sensor's XY plane. We define the angle with respect to the vertical as the angle between the lab's Z axis and the sensor's Y axis, indicated here as θ .

Figure 2: The gold-standard (GS) angles and IMU angles at (a) T1 (RMSE = 3.04°), (b) T7 (RMSE = 1.02°), (c) L1 (RMSE = 0.71°), and (d) S2 (RMSE = 3.57°). This was for a stroke rate of 20 strokes per minute for one participant.

Figure 3: The gold-standard (GS) angles and IMU angles at (a) T1 (RMSE = 3.51°), (b) T7 (RMSE = 1.04°), (c) L1 (RMSE = 0.73°), and (d) S2 (RMSE = 3.54°). This was for a stroke rate of 24 strokes per minute for one participant.

Figure 4: The gold-standard (GS) angles and IMU angles at (a) T1 (RMSE = 3.65°), (b) T7 (RMSE = 1.10°), (c) L1 (RMSE = 0.83°), and (d) S2 (RMSE = 2.97°). This was for a stroke rate of 28 strokes per minute for one participant.

Figure 5: The gold-standard (GS) angles and IMU angles at (a) T1 (RMSE = 3.17°), (b) T7 (RMSE = 1.07°), (c) L1 (RMSE = 0.91°), and (d) S2 (RMSE = 3.65°). This was for a stroke rate of 32 strokes per minute for one participant.